

# BENCHMARK AND THRESHOLD ANALYSIS OF LONGITUDINAL INSTABILITY IN THE PSR\*

S. Cousineau, J. Holmes, ORNL, Oak Ridge, USA

C. Beltran, R. Macek, Los Alamos Neutron Science Center † Los Alamos, NM, USA

## Abstract

A set of inductive inserts used to provide passive longitudinal space charge compensation in the Los Alamos Proton Storage Ring cause a strong longitudinal instability in the beam when the inductors are at room temperature. We use the ORBIT code to perform benchmarks of the instability dynamics, including the mode spectrum and the instability growth time. Additionally, we analyze the experimental instability intensity threshold and compare it with the simulated threshold. For all parameters benchmarked, results from simulations are in good agreement with the experimental data.

## INTRODUCTION

The Proton Storage Ring (PSR) is the accumulator ring portion of the Los Alamos Neutron Science Center (LAN-SCE), a 100 kW proton driver used for neutron spallation. In order to satisfy low beam loss requirements during high intensity operations, the PSR must maintain a clean beam gap to accommodate extraction kicker rise and fall fields. In 1999 three inductive inserts were placed in the ring to provide passive longitudinal space charge compensation. Though the inductors were shown to be effective in reducing the beam in the gap, they also caused an unacceptably large longitudinal instability, and were thus removed from the ring. Later the same year, two of the inductors were reintroduced into the ring, this time heated to 125 degrees Celsius, which resolved the instability. The PSR machine now operates with two heated inductors and does not suffer from the instability during normal operation.

The ORBIT code is a particle-in-cell tracking code developed for realistic modeling of beams in rings and transport lines [2, 3]. A primary use of ORBIT is in the design and optimization of future high intensity machines. It is therefore of particular importance to benchmark the code's algorithms which model collective effects with existing experimental data. In this work, we benchmark ORBIT's longitudinal space charge and impedance model against the PSR longitudinal instability. We compare the mode spectrum and the growth time of the instability, and additionally perform an analysis and benchmark of the intensity instability threshold. Two separate data sets are studied: One

with three room temperature inductive inserts in the ring, and the other with two room temperature inductive inserts.

## BENCHMARK OF PROFILE DATA, MODE SPECTRUM, AND GROWTH TIME

### Experimental Data

In the experiment presented in this section, 650 nC of charge was accumulated in 150  $\mu$ s, and then stored for another 350  $\mu$ s. No RF bunching was applied, and three room temperature inductive inserts were present in the ring. A complete set of machine conditions, along with analysis of the experimental data, can be found in reference [1]. Here we only restate the results of this analysis.

Figure 1 shows two consecutive turns of a wall current monitor signal at the end of beam injection into the ring (150  $\mu$ s), and at the peak of the instability (350  $\mu$ s). The hash at the top of the first plot (Figure 1(a)) corresponds to the linac 201 MHz microbunch structure. The instability is visible as the large spikes in the profile in Figure 1(b), which occur at a frequency of 72 MHz. For the PSR with revolution frequency of 2.8 MHz, the unstable harmonic is closest to  $h=26$ . The experimental growth time for the instability in this data set was found in reference [1] to be 33  $\mu$ s.

### ORBIT Simulations

To simulate the experiment shown in Figure 1, we invoke ORBIT's 1D tracking package, which includes an algorithm for modeling the effects of longitudinal space charge and user-defined external impedances. One combined space charge and impedance kick is applied per turn of the beam, adequate for modeling the slow longitudinal evolution of the PSR beam. Numerical convergence is achieved by slicing the beam into 256 bins, and using  $8 \times 10^6$  macroparticles.

The impedance of the room temperature inductive inserts was measured in reference [1], and is reproduced here in Figure 2. Note that both the real and imaginary parts peak in the range of 70-80 MHz.

Using this impedance and the experimental parameters given in the previous section, the ORBIT code was used to simulate the instability observed in Figure 1. To allow for direct comparison of experimental and simulated profiles, the simulated turn-by-turn longitudinal profiles are plotted with the same resolution as the wall current monitor data (0.5 ns). The results are shown in Figure 3, where the first

\*SNS is managed by UT-Battelle, LLC, under contract DE-AC05-00OR22725 for the U.S. Department of Energy. SNS is a partnership of six national laboratories: Argonne, Brookhaven, Jefferson, Lawrence Berkeley, Los Alamos, and Oak Ridge.

† The Los Alamos National Laboratory is operated by the University of California for the U.S. DOE under contract W-7405-ENG-36.

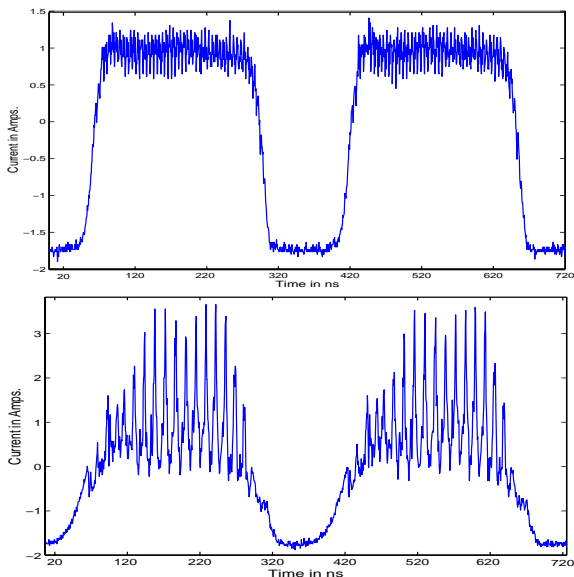


Figure 1: a) Two-turn wall current monitor signal at the end of injection. b) Two-turn wall current monitor signal at the peak of the instability.

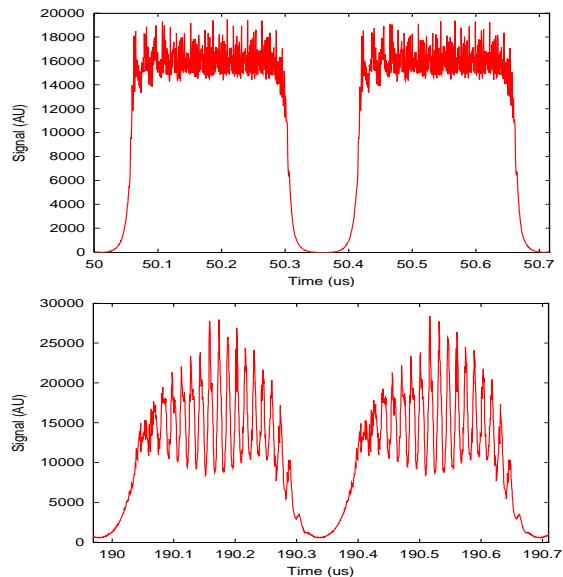


Figure 3: a) Simulated two-turn wall current monitor signal at the end of injection. b) Simulated two-turn wall current monitor signal at the peak of the instability.

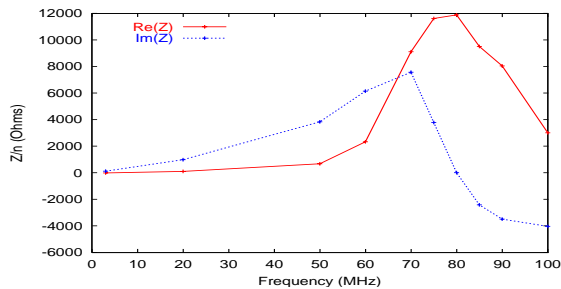


Figure 2: The measured real and imaginary part of the impedance for the three ferrite inductors at room temperature.

plot shows two consecutive turns at the end of beam injection (Figure 3(a)), and the second plot shows two consecutive turns at the peak of the instability (Figure 3(b)). The same basic structure is seen in the simulated profiles as in the experimental profiles, and the peak of the simulated instability occurs within a few microseconds of the experimental peak.

To complete the benchmark, we analyze the mode spectrum of the instability by tracking the evolution of the dominant harmonics throughout the beam injection and storage. The result is shown for the three most dominant harmonics, all of which exhibit an exponential growth pattern, in Figure 4(a). In agreement with the experimental result, the dominant harmonic is  $h=26$ . Taking the natural log of the  $h=26$  evolution curve and fitting a slope to the straight part of the curve (Figure 4(b)), we derive a growth time of  $42 \mu s$  for the simulated instability, which is about 25% slower than the experimental result.

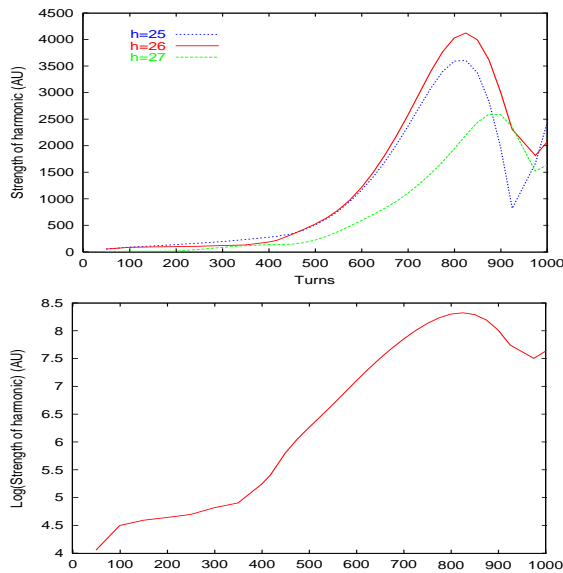


Figure 4: a) Evolution of the three most dominant harmonics during the beam injection and storage. b) The natural log of the  $h=26$  harmonic curve shown in (a).

### ANALYSIS AND BENCHMARK OF INSTABILITY INTENSITY THRESHOLD

In addition to the 1999 data set shown in the previous section, another data set was taken in 2002 to study the instability intensity threshold. Only two room temperature inductors were present in the ring during this study, and the instability is slightly weaker than what was observed in the previous section. However, the quality of the data and the strength of the instability are more than sufficient to identify the threshold.

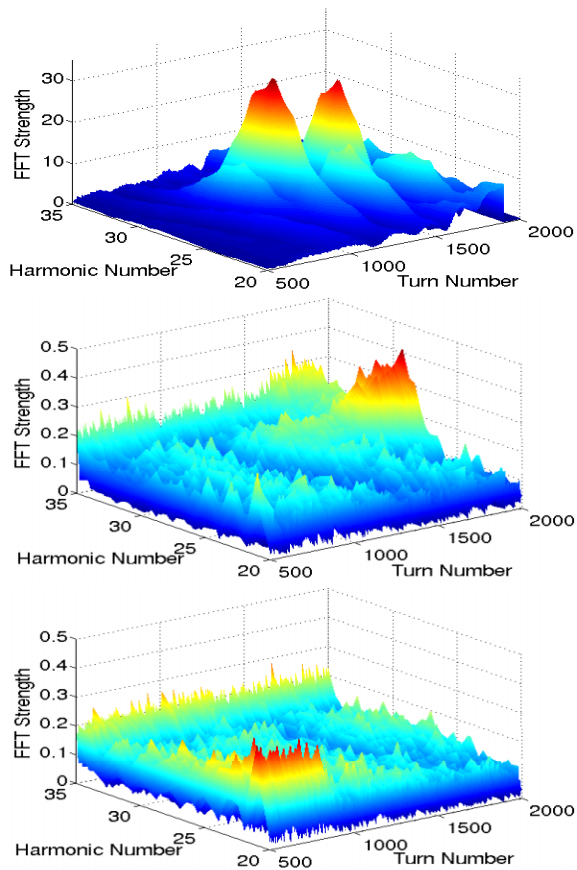


Figure 5: a) Mode evolution plot from the end of injection to the end of storage for a 460 nC chopped beam. b) The same for a 80 nC beam. c) The same for a 70 nC beam.

For these experiments, a 200 ns chopped beam was accumulated in the ring for 200  $\mu$ s and then stored with no RF bunching for an additional 500  $\mu$ s. Multiple data sets were taken, varying the intensity from 70 nC to 460 nC. The data was imported into MATLAB for analysis, and the evolution of the instability was analyzed by plotting the evolution of the mode spectrum over the injection and storage period.

To identify the intensity instability threshold, it is necessary to state the defining behavior of the beam at the point of threshold. For this study, we define the threshold as the intensity at which the unstable harmonics rise coherently above the noise level. Figure 5 shows the mode evolution plots for three different beam intensities in the experimental data set: 460 nC, 80 nC, and 70 nC. At 460 nC a very strong instability is observed; at 80 nC the relevant harmonics are just beginning to rise out of the noise; and, finally, at 70 nC only noise is observed. Therefore, according to our definition, the experimental instability intensity threshold is around 80 nC.

As a final benchmark of the ORBIT code, we simulated the threshold study experiments and analyzed the simulated data with the same method as the experimental data. The results are shown in Figure 6. Here, we see that at 500 nC a very strong instability is present; at 70 nC the relevant

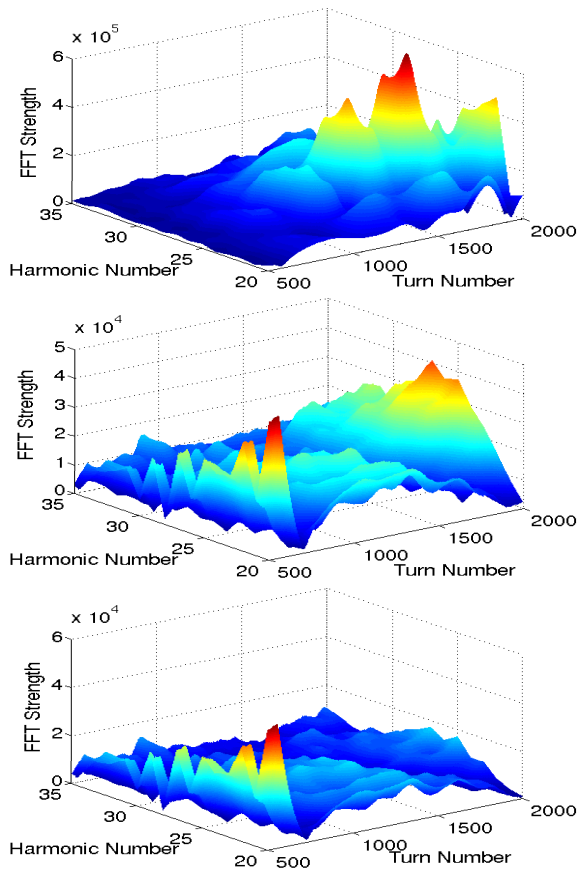


Figure 6: a) Simulated mode evolution plot from the end of injection to the end of storage for a 500 nC chopped beam. b) The same for a 70 nC beam. c) The same for a 50 nC beam.

harmonics are just beginning to rise out of the noise; and, finally, at 50 nC only noise is observed. Therefore, the simulated threshold is around 70 nC, within 25% of the experimental threshold.

## REFERENCES

- [1] C. Beltran, *Study of the Longitudinal Space Charge Compensation and Longitudinal Instability of the Ferrite Inductive Inserts in the Los Alamos Proton Storage Ring*, Ph.D. thesis, Indiana University, 2004, unpublished.
- [2] J. Galambos, J. Holmes, A. Luccio, D. Olsen, and J. Beebe-Wang, *ORBIT Users Manual*, <http://www.sns.gov/APGroup/Codes/Codes.htm>.
- [3] J. Holmes, S. Cousineau, J. Galambos, A. Shishlo, Y. Sato, W. Chou, M. Michelotti, F. Ostiguy, *ICFA Beam Dynamics Newsletter No. 30*, 100 (2003).